CommonOcean: Composable Benchmarks for Motion Planning on Oceans

Hanna Krasowski and Matthias Althoff

***Abstract*— Autonomous vessels can increase safety and reduce emissions compared to human-operated vessels. One important task for autonomous vessels is motion planning. Currently, there are no benchmarks for autonomous vessels to compare different motion planning methods. Thus, we introduce composable benchmarks for motion planning on oceans (CommonOcean), which is available at `commonocean.cps.cit.tum.de`. A CommonOcean benchmark consists of three elements: cost function, vessel model, and motion planning scenario. Benchmarks can be conveniently composed using unique identifiers for these elements, which are highly modular. CommonOcean is easy to use, because we provide meaningful parameters for vessel models, various motion planning scenarios, and comprehensive documentation. Furthermore, we developed a scenario generation tool, which allows one to effortlessly create new scenarios from marine traffic data. We believe that CommonOcean will lead to a better reproducibility and comparability of research on motion planning for vessels.**

I. Introduction

Seaborne trade is responsible for transporting more than 80 percent of the global trade volume; thus, it is a critical component of our globalized economy [1]. This was demonstrated by the MV Ever Given incident in 2021 [2]. Because most marine accidents are caused by human error [3], autonomous vessels have a high potential of increasing the safety and efficiency of vessels.

Motion planning is an important task for autonomous vessels. Automatic identification system (AIS) data contains all information for extracting realistic benchmarks for motion planning problems of vessels and AIS data is publicly receivable via radio. However, most vessel movements recorded by AIS are uncritical. Thus, there is a need for a meaningful scenario generation to avoid trivial motion planning tasks. Additionally, the scenario representation should be comprehensive for capturing the breadth of marine traffic situations.

Motion planning tasks of vessels have been solved using different methods, such as reinforcement learning [4]–[6], sampling-based methods [7], [8], or optimization-based methods [9]. At this time, published motion planners for vessels cannot be compared because of the unavailability of public and standardized benchmarks. Even reproducing the results of a published motion planner is often impossible, because page limitations prevent authors from providing all the required information.

We used our experience from CommonRoad [10] for motion planning on roads to develop the first benchmarking suite for motion planning on oceans: CommonOcean. The concept of CommonOcean is similar to that of CommonRoad. This eases re-using motion planners developed for road vehicles for vessels and might attract autonomous driving researchers to test their planners on maritime applications. The key features of CommonOcean are as follows:

- *Composability* – The tool is designed so that scenarios, vessel models, and cost functions can be changed and adapted independently of the other components.
- *Repeatability* – We provide all necessary software to reproduce benchmarks and a comprehensive documentation to ease usability.
- *Independence* – The scenario representation can be used independently of specific motion planners.
- *Openness* – All benchmarks are freely available and we provide open-source software to generate new scenarios from AIS data.

The remainder of this study is structured as follows: In Section II, we discuss the related work on benchmarks for intelligent transportation systems and software tools for autonomous vessels. In Sections III - VI, we introduce the benchmark terminology and its components: cost functions, vessel models, and our scenario representation. In Section VII, we outline our acquisition of benchmarking scenarios in detail. Finally, we provide an example benchmark with a motion planning solution in Section VIII and conclude the study in Section IX.

II. Related Work

There are benchmarking suites for motion planning tasks for autonomous driving [10], [11], robotic manipulators [12], [13], and general motion planning tasks [14]. Our previous work proposed CommonRoad [10] – a benchmarking suite for any type of motion planner that provides numerous benchmark scenarios for autonomous driving. CommonRoad provides traffic scenarios with pedestrians, cyclists, and different road vehicles. Vinitsky et al. [11] introduced eleven interactive autonomous driving benchmarks for reinforcement learning agents. Fan et al. [12] provided benchmarks for reinforcement learning on robotic manipulation tasks. Similarly, James et al. [13] presented a reinforcement learning environment next to a benchmarking suite for different tasks in vision-guided robotic manipulation. Moll et al. [14] proposed a tool to define benchmarks for different motion planning problems for the *Open Motion Planning Library*[1].

Generally, there are fewer scientific software tools for motion planning of autonomous vessels than for autonomous

All authors are with the Department of Informatics, Technical University of Munich, 85748 Garching, Germany.
{hanna.krasowski, althoff}@tum.de

[1] `ompl.kavrakilab.org`

driving [15]–[18]. However, some open-source tools support the research and development of autonomous vessels. For example, *Bridge Command*[2] is a simulator for the bridge of a vessel that facilitates navigation training, radar usage, and other seamanship skills. The *sail-pro*[3] tool provides a virtual environment for sailing ships. The *Marine Systems Simulator (MSS)*[4] is a MATLAB library for vessels, which includes dynamical models and parameters for different vessel types. Finally, Kidd [19] presented a method for building a small autonomous vessel for research and provided an open-source software stack to deploy it. However, to the best of our knowledge, no tools provide versatile and modular benchmarks for motion planning on waters.

III. Composable benchmarks

Our benchmark specification is composed of a scenario, vessel model, and cost function. The scenario consists of obstacles, restricted water areas, traffic signs, traffic rules, and a planning problem for the ego vessel, i.e., the vessel we control. The state of the ego vessel at time t is $x(t) \in \mathbb{R}^n$ and its initial state is $x_{0,S}$. The vessel model M determines the dynamics for the ego vessel by a state space model, i.e., $\dot{x}(t) = f_M(x(t), u(t))$, where $u(t) \in \mathbb{R}^m$ is the control input. The cost function $J_C(x(t), u(t), t_0, t_f)$, with the initial time t_0 and the final time t_f, determines how the planned trajectory should be evaluated. The objective of the ego vessel is to reach the goal region $\mathcal{G}_S \subset \mathbb{R}^n$ at t_f.

We use the same format to specify benchmark B as for CommonRoad [10, Sec. II]:

$$\mathrm{B} = \mathrm{M} : \mathrm{C} : \mathrm{S},$$

where M specifies the vessel model, C is the cost function, and S is the scenario. The benchmarking objective is to solve the motion planning problem and obtain the optimal control input trajectory $u^*(\cdot)$ such that the cost J_C is minimized. Note that $(\cdot)$ abbreviates all time steps from t_1 to t_f. Furthermore, the constraints for the motion planning problem must be respected. This implies that the ego vessel follows its dynamics, the ego vessel only occupies the freely navigable space $\mathcal{W}_{\mathrm{S},\mathtt{free}}(t) \subset \mathbb{R}^3$, and additional constraints $(g_S(x(t), u(t), t) \leq 0)$ such as traffic rules. We obtain the occupancy of a vessel in state $x(t)$ using the function $O(x(t)) : \mathbb{R}^n \to P(\mathbb{R}^3)$, where $P(\mathcal{S})$ returns the power set of a set $\mathcal{S}$. The motion planning problem is formally defined as [10, Eq. (2)]:

$$u^*(\cdot) = \underset{u(\cdot)}{\arg\min}\ J_C(x(t), u(t), t_0, t_f) \tag{1}$$

subject to

$$\begin{aligned} &\dot{x}(t) = f_M(x(t), u(t)), \quad O(x(t)) \in \mathcal{W}_{\mathrm{S},\mathtt{free}}(t), \\ &g_S(x(t), u(t), t) \leq 0, \quad x(t_0) = x_{0,S}, \quad x(t_f) \in \mathcal{G}_S, \end{aligned}$$

where $u(\cdot)$ is a control input trajectory candidate.

[2] bridgecommand.co.uk
[3] github.com/rururu/sail-pro
[4] github.com/cybergalactic/MSS

IV. Cost Functions

To foster synergies between motion planning on roads and waters, we use the same format as in CommonRoad for the cost function. This will make it easier to adjust motion planners designed for motion planning on roads to apply to vessels as well. The overall cost function for a benchmark consists of several weighted components [10, Sec. IV]:

$$J_C(x(t), u(t), t_0, t_f) = \sum_{i \subset \mathcal{I}} w_i J_i(x(t), u(t), t_0, t_f),$$

where $\mathcal{I} \subset \mathcal{P}$ contains the identifiers of the applied cost components, $\mathcal{P}$ is the set of all partial cost identifiers, and $w_i \in \mathbb{R}^+$ are the weights for the cost functions. For example, to specify a cost function from the partial costs time J_T, acceleration J_A, and yaw rate J_Y (defined in [10]) with weights $w_T = 0.5$, $w_A = 1.0$, and $w_Y = 0.8$, respectively; the short notation is $[(T|0.5), (A|1.0), (Y|0.8)]$.

From the cost components for motion planning on roads presented in [10], all cost components except for the lane center offset J_{LC}, steering angle J_{SA}, and steering rate cost J_{SR} can be re-used for vessels. The lane center offset J_{LC} is unmeaningful for vessels as there are no lanes for vessels. Only occasionally there are traffic separation zones or marked waterways where vessels must navigate close to the borders of these areas. The cost components for the steering angle J_{SA} and the steering rate J_{SR} can be adapted to the rudder angle J_{RA} and rudder turning rate J_{RR}:

- **Rudder angle**: $J_{RA} = \int_{t_0}^{t_f} \beta(t)^2 \delta t$,
- **Rudder turning rate**: $J_{RR} = \int_{t_0}^{t_f} v_\beta(t)^2 \delta t$,

where $\beta(t)$ is the rudder angle at time t, and $v_\beta(t)$ is the rudder turning rate. Note that we define all variables in SI units.

We introduce two additional components next to the adjusted road vehicle cost functions. First, the rule compliance cost evaluates if the vessel complied with all formalized rules R_1 to R_6 [20] from the Convention on the International Regulations for Preventing Collisions at Sea (COLREGS) [21]. This is usually integrated as a hard constraint (i.e., $J_R = 0$), but can be recast to a soft constraint. Second, the criticality cost evaluates the criticality between the ego vessel and all other vessels in the scenario using the vessel conflict ranking operator (VCRO) [22, Eq. (22)]. We define these costs as follows:

- **Rule compliance**: $J_R = \begin{cases} 1 & \neg(R_1 \wedge ... \wedge R_6) \text{ [20]}, \\ 0 & \text{otherwise}, \end{cases}$
- **Criticality**: $J_{VC} = \sum_{o \in \mathcal{O}} \int_{t_0}^{t_f} \mathrm{VCRO}(x(t), x_o(t)) \delta t$ [22],

where $\mathcal{O}$ is the set of other vessels and R_i is true when the vessel complies with rule R_i.

V. Vessel Models

Different dynamical models are used for vessels depending on the degree of detail required for a specific problem.

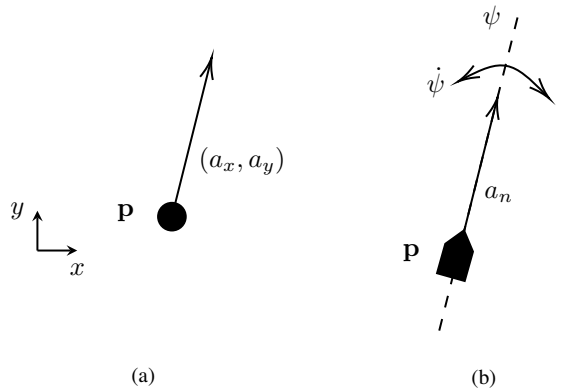

Fig. 1. Visualization of the control inputs and state for (a) the velocity-constrained point mass model and (b) the yaw-constrained model.

We specify three common vessel models from maneuvering theory [23], where the goal of the ego vessel is to maneuver along a specified reference path or toward a goal area. For all vessel models, we ignore the earth's curvature and assume the water surface to be a two-dimensional plane. This is not a restriction in practice because the motion planning problem is reset frequently for a limited time horizon. Our unique model identifiers are built from the model type (e.g., YP for yaw-constrained point mass) followed by a number, which refers to the parameters of a specific vessel. The vessel associated with a specific number is documented in the *vessel models*[5] repository.

A. Velocity-Constrained Point Mass Model (VP)

The velocity-constrained point mass model is shown in Fig. 1 (a) and is used for motion planning in compliance with the COLREGS [24] or reinforcement learning [5] because of its simplicity. For this model, the vessel is reduced to a single point with position $\mathbf{p} = [p_x, p_y]^T \in \mathbb{R}^2$, velocity $\mathbf{v} = [v_x, v_y]^T \in \mathbb{R}^2$, and acceleration input $\mathbf{a} = [a_x, a_y]^T \in \mathbb{R}^2$. All values are obtained in a world-fixed frame; thus, we obtain the following model:

$$\begin{aligned} \dot{p}_x = v_x,\ \dot{p}_y = v_y,\ \dot{v}_x = a_x,\ \dot{v}_y = a_y, \qquad (2)\\ \text{subject to} \sqrt{a_x^2 + a_y^2} \leq a_{max},\\ \sqrt{v_x^2 + v_y^2} \leq v_{max}, \end{aligned}$$

where a_{max} is the physical limit for the vessel's acceleration and v_{max} is the maximal velocity. The model realizes motions in arbitrary directions instantaneously, thus, ignoring the nonholonomic behavior of most vessels in motion.

B. Yaw-Constrained Model (YP)

In reality, the turning motion of a vessel is more constrained than for the velocity-constrained point mass model. For example, a vessel cannot navigate sideways when it is equipped only with a propeller at the stern and no external forces are acting on it. The yaw-constrained model (see Fig. 1 (b)) mitigates this problem by constraining the rotational movement of the vessel. This is inspired by [4]; however, the study only specifies a time-discrete model and uses the surge as the control input instead of the acceleration, which is less realistic as the velocity cannot instantaneously change.

The vessel model's state space consists of the position of the vessel $\mathbf{p}$, heading $\psi \in \mathbb{R}$, and the velocity $n \in \mathbb{R}$, which is aligned the orientation of the vessel and also called surge. The control values are the longitudinal acceleration $a_n \in \mathbb{R}$ and the yaw rate $\omega \in \mathbb{R}$. The dynamics of this model are given as follows:

$$\begin{aligned} \dot{p}_x = \cos\psi\, n,\ \dot{p}_y = \sin\psi\, n,\ \dot{\psi} = \omega,\ \dot{n} = a_n, \qquad (3)\\ \text{with } a_n \in [a_{n,min}, a_{n,max}] \text{ and } \omega \in [\omega_{min}, \omega_{max}]. \end{aligned}$$

C. Three Degrees of Freedom Model (3F)

Both previously presented models do not capture environmental influences. Additionally, the dynamic constraints of a real vessel can only be roughly captured. For example, the acceleration limit over velocity is roughly a bell curve, i.e., the acceleration limit is high for medium velocities. Thus, we present the three degrees of freedom model from [23], which includes environmental influences and more realistic dynamical constraints.

The vessel model's state consists of the position and orientation $\boldsymbol{\eta} = [p_x, p_y, \psi]^T \in \mathbb{R}^3$ and the velocities $\boldsymbol{\nu} = [n, v, \omega]^T \in \mathbb{R}^3$, where v is the lateral velocity (also called sway). We express $\boldsymbol{\eta}$ and $\boldsymbol{\nu}$ in the global and vessel-fixed reference frame, respectively. The transformation between the two state representations is defined using the rotation $\boldsymbol{R}(\psi)$ [23, Eq. (7.4)]:

$$\dot{\boldsymbol{\eta}} = \boldsymbol{R}(\psi)\boldsymbol{\nu} = \begin{bmatrix} \cos\psi & -\sin\psi & 0 \\ \sin\psi & \cos\psi & 0 \\ 0 & 0 & 1 \end{bmatrix} \boldsymbol{\nu}. \qquad (4)$$

For the three degrees of freedom model, Fossen [23] assumes that the vessel has a homogeneous mass distribution and that the port and starboard sides are symmetric. Furthermore, the origin of the vessel-fixed reference frame is set to the center of gravity for the vessel.

The control input $\boldsymbol{\tau} = [F_x, F_y, M_n]^T \in \mathbb{R}^3$ consists of the force F_x along the x-axis, force F_y along the y-axis, and the angular moment M_n around the z-axis of the body-fixed reference frame. Note that the rudder or propeller is not modeled directly. Instead their effects on the vessel are collected through $\boldsymbol{\tau}$. If desired, $\boldsymbol{\tau}$ can be substituted by a model for the rudder and propeller dynamics as described in [25]. A method to include wind and wave forces is described in detail in [26]. However, they are often negligible for motion planning and can be set to zero. Thus, we omit them for the three degrees of freedom model.

Combining the dynamics of the rigid body and hydrodynamic forces, the three degrees of freedom model can be

[5]available at `commonocean.cps.cit.tum.de`

described using [23, Eq. (7.5)]:

$$\boldsymbol{M}\dot{\boldsymbol{\nu}} + \boldsymbol{C}(\boldsymbol{\nu})\boldsymbol{\nu} + \boldsymbol{D}\boldsymbol{\nu} = \boldsymbol{\tau}, \tag{5}$$

with

$$\boldsymbol{M} = \boldsymbol{M}_{RB} + \boldsymbol{M}_{A}, \tag{6}$$

$$\boldsymbol{C}(\boldsymbol{\nu}) = \boldsymbol{C}_{RB}(\boldsymbol{\nu}) + \boldsymbol{C}_{A}(\boldsymbol{\nu}), \tag{7}$$

where the rigid-body mass is $\boldsymbol{M}_{RB} \in \mathbb{R}^{3\times3}$, the added hydrodynamic mass is $\boldsymbol{M}_{A} \in \mathbb{R}^{3\times3}$, the rigid-body Coriolis-centripetal matrix is $\boldsymbol{C}_{RB}(\boldsymbol{\nu}) \in \mathbb{R}^{3\times3}$, the hydrodynamic Coriolis-centripetal matrix is $\boldsymbol{C}_{A}(\boldsymbol{\nu}) \in \mathbb{R}^{3\times3}$, and the linear damping is modeled using $\boldsymbol{D} \in \mathbb{R}^{3\times3}$. We omit the parameters for the matrices and refer the interested reader to [23] and our *vessel models* repository. For the presented model, 20 parameters must be identified already. Some of these parameters, such as the mass or inertia components, are known from the construction of the vessel. Other parameters, such as the coefficients for the damping forces, can be determined experimentally [27], [28].

VI. Scenario Representation

To easily adapt motion planners developed for road vehicles, we intentionally use a similar representation for scenarios as in CommonRoad [10]. Our scenarios contain navigable waters, obstacles, and traffic signs. Furthermore, we store auxiliary information about the benchmark, such as the data source, GPS coordinates, day, time, and sea state. Fig. 2 shows the structure of the XML files that represent these scenarios. We provide comprehensive XML and scenario documentation as well as a scenario database on the CommonOcean website.

A. Waters

In contrast to road traffic, maritime traffic is usually less structured and only for some areas there are navigational restrictions. Thus, we first delimit the scenario area to a rectangular area. If only this is specified, the whole scenario area is navigable by all kinds of vessels. Additionally, we also specify restricted waters such as traffic separation zones, marked waterways, and shallows. Waters are delimited by a left and right bound (waterways and traffic separation zones) or by a polygon (shallow). For shallows, we additionally define the maximal draft for a vessel to safely navigate such areas.

B. Traffic Signs

CommonOcean currently supports the most prominent traffic signs, which are lateral, cardinal, and special marks (see Fig. 3). In contrast to road traffic signs, which are placed next to roads, traffic signs on the water must be considered static obstacles for maritime traffic. Therefore, the traffic signs are also static obstacles, while we differentiate between swinging traffic signs, such as buoys, and static traffic signs, such as static poles. For buoys, the static obstacle is extended to the reachable area of the buoy, whereas for static traffic signs, the spatial dimensions of the static obstacle match the dimensions of the traffic sign.

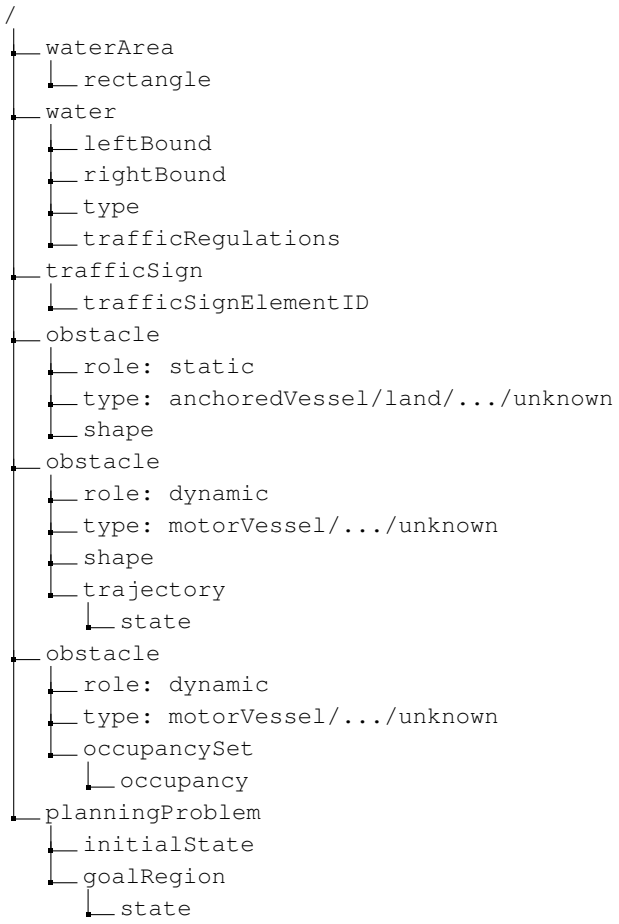

Fig. 2. Structure of the XML files encoding each scenario.

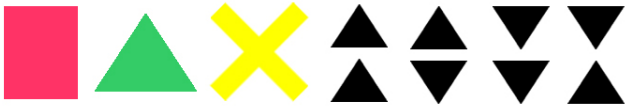

Fig. 3. Visualization of supported traffic signs. From left to right: two lateral marks, special mark, and cardinal marks for north, east, south, and west.

C. Obstacles

Obstacles are defined by their role (static, or dynamic), type (motorVessel/sailingVessel/fishingVessel/militaryVessel/cargoShip/vesselNotUnderCommand/anchoredVessel/restrictedManeuverabilityVessel/windfarm/oilrig/buoy/land/shallow/unknown), shape (rectangle, circle, or polygon), and movement over time in case the obstacle is dynamic. Most of the vessels can be closely approximated by a rectangle. A polygon can be used if the spatial dimensions of the vessel should be more detailed. For wind wheels in wind farms and swinging buoys, circles are a good approximation. Land areas are represented as static obstacles through polygons. For motion planning of a vessel, the vessel's draft is also important. Thus, the obstacle shapes are accompanied by a depth specification, while `inf`

indicates that the obstacle is connected to the sea bottom. The vessel's movement over time can be represented using the same classes as for CommonRoad [10], i.e., trajectories of states for known behavior, occupancy sets for unknown behavior, and probability distributions of states for unknown stochastic behavior.

D. Planning Problem

Furthermore, each scenario contains a planning problem, which specifies the initial state and the goal region for the ego vessel. There can be one or multiple goal regions specified by a point or shape (rectangle, circle, or polygon). Additionally, an orientation, time and velocity interval can be defined to further tighten the goal definition. For some motion planning problems, vessels should not follow a straight path from the initial state to the goal region, e.g., in narrow channels. Then, the goal definition can be extended with ordered waypoints and a maximal deviation from the path, which the waypoints describe.

VII. Scenario Generation

AIS data is a massive data source for generating motion planning tasks as approximately 200 000 vessels are tracked every day by major AIS data providers, such as marine traffic[6]. All commercial vessels with a gross tonnage of more than 300 and all passenger vessels must have AIS on board. Particularly, on the open sea, one can assume that AIS data captures all vessels. AIS data consists of static, dynamic, and voyage information. Thus, AIS data contains all information necessary for generating dynamic obstacles and planning problems for CommonOcean.

Tu et al. [29] compared different AIS data sources. The Marine Cadastre dataset [30] is a public data source with high precision and good time resolution, which has been providing historic AIS data of the United States coastal waters since 2009. Currently, this dataset is our main source for CommonOcean scenarios. We implement the benchmark generation in a two-step process. First, we use AIS data to generate dynamic obstacles and a planning problem. Then, we convert the sea map for the geographic location to waters, static obstacles and traffic signs. The results of both steps are combined and stored in an XML scenario file. The *dataset converters*[7] repository provides the source code for this scenario generation.

A. Situation Selection

The simplest possibility of generating dynamic obstacles and planning problems is extracting these from AIS data for a specific time frame and geographic region. The user must specify the following: start and end time, GPS coordinates that describe the geographic region as a box, number of planning problems to be generated, and desired time discretization. Then, the AIS data is filtered according to the user input and all extracted vessels are converted to dynamic obstacles. A dynamic obstacle trajectory of a vessel is linearly interpolated when AIS data is missing for the specified time discretization. Finally, planning problems are generated by removing dynamic obstacles and generating planning problems from their initial state, final state, and shape, whereby the final state and the shape of the vessel are used to specify the goal region.

The second possibility of generating benchmarks is to extract close encounters of vessels in a specified geographical region. This scenario selection approach is inspired by the data generation in [20] and is particularly useful for extracting interesting open sea situations because vessels rarely encounter other vessels on the open sea. In addition to the information for the first approach, the user must specify the maximal distance and minimal time duration for an encounter. From the found encounters, dynamic obstacles and their trajectories are generated. Finally, the planning problems are generated in the same manner as the first approach.

B. Sea Map Conversion

For open sea scenarios, map conversion is often unnecessary as there are no static obstacles or traffic signs that restrict the motion planning. However, we integrate the corresponding sea map into the scenario if the scenario is not on the open sea. Thus, we developed a map conversion for OpenSeaMap[8], which is based on the OpenStreetMap conversion from the CommonRoad Scenario Designer [31]. Fig 4 depicts an exemplary conversion for a scenario on the New York coast.

VIII. Example

We demonstrate benchmarking motion planning for vessels on the simple but realistic scenario `USA_MEC-1_20190129_T-22`, which was recorded for the US coast on January 29th, 2019. The AIS data is from the Marine Cadastre dataset. We detected this situation using the second mode of scenario generation, where close encounters of vessels are extracted from a predefined geographic region. In this AIS scenario, three vessels encountered each other and we removed one to generate the planning problem. The center of the scenario coordinate system is at $38.730\,57°$ North and $74.979\,77°$ West; the goal of the scenario must be reached within $t_f \in [38.3\text{min}, 45\text{min}]$; and the time step size is $10\,\text{s}$.

We used an A*-search-based trajectory planner with motion primitives generated using the velocity-constrained point mass model (see in Section V-A) and the parameters for a container vessel ($VP1$) to solve the motion planning task. The cost function consists of an acceleration cost (J_A), final time cost (J_T), and cost for COLREGS compliance (J_R):

$$J_{SB1}(x(t), u(t), t_0, t_f) = w_T J_T + w_A J_A + w_R J_R.$$

A low cost indicates low accelerations, a short time necessary to solve the scenario, and compliance with the COLREGS. The weights are $[(T|0.1), (A|0.5), (R|200)]$.

[6] `marinetraffic.com`

[7] available at `commonocean.cps.cit.tum.de`

[8] `openseamap.org`

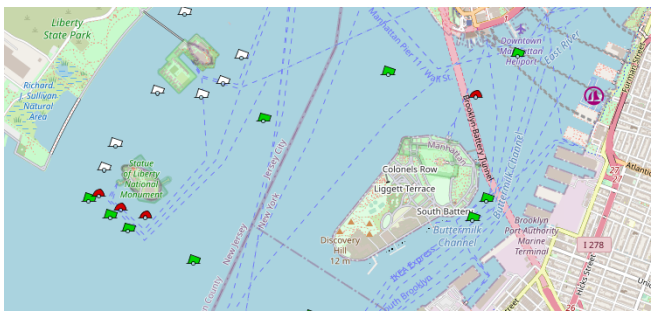

(a) OpenSeaMap map of the scenario.

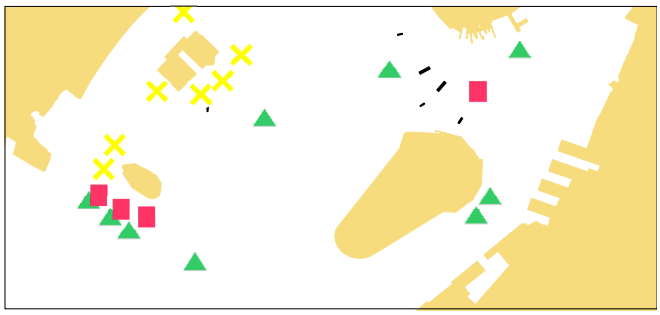

(b) CommonOcean scenario with black vessels and traffic sign symbols (see Fig. 3).

Fig. 4. Scenario `USA_NYM-1_20190613_T-1` generated from AIS data of New York, USA.

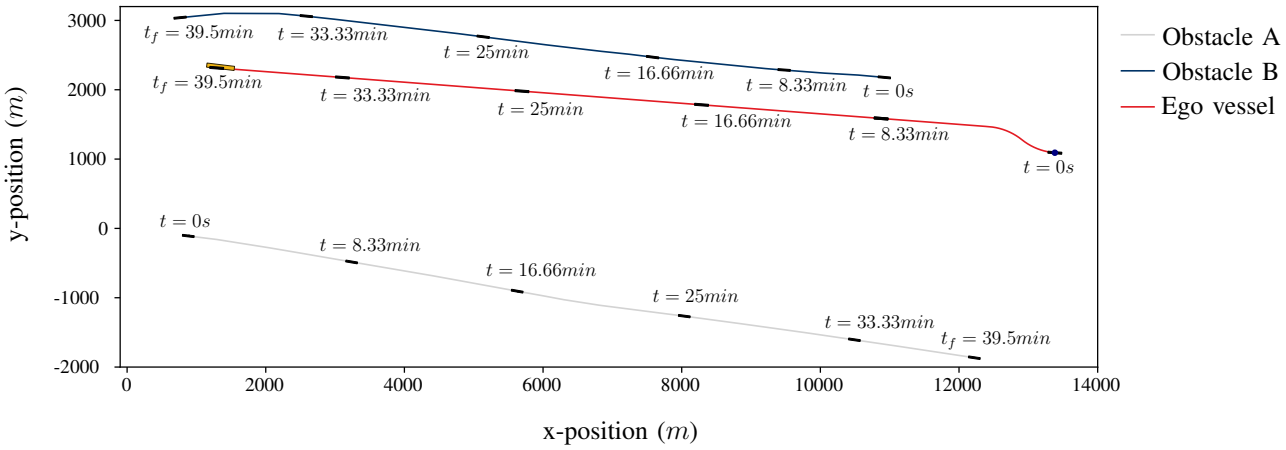

Fig. 5. Example trajectory solution for benchmark `VP1:SB1:USA_MEC-1_20190129_T-22`. The goal region is depicted in orange and the initial state of the planning problem is a blue circle.

The unique identifier for the benchmark is $B = VP1 : SB1 : USA\_MEC - 1\_20190129\_T - 22$ and the planned trajectory has a cost of $J_{SB1} = 237.097$. Fig. 5 depicts the benchmark scenario and the planned trajectory.

IX. Conclusions

We introduced CommonOcean, which is an open-source benchmarking suite for motion planning of surface vessels. We define the necessary components for benchmarking, i.e., a cost function, a vessel model, and a scenario including a planning problem. These components are highly modular while at the same time they briefly specify the exact benchmarking setting. Furthermore, we provide data conversion tools, which ease creating new benchmarks from AIS data. The full source code, detailed documentation, and tutorials are accessible from **commonocean.cps.cit.tum.de**. We hope that the research community will use and possibly extend this toolbox for better comparability and repeatability of research on motion planning for vessels. In addition to maintaining CommonOcean, we plan to publish the following functionalities in the future:

- extend the data converters to more AIS data sources, i.e., AISHub[9] and more national sources, such as the Danish Maritime Authority[10];
- provide highly challenging benchmarks, e.g., generated from vessel collisions;
- add baseline motion planner implementations;
- integrate weather data sources and more sea map sources in the scenario generation and representation.

Acknowledgment

The authors gratefully acknowledge the partial financial support of this work by the research training group ConVeY funded by the German Research Foundation under grant GRK 2428 and by the project TRAITS funded by the German Federal Ministry of Education and Research.

[9] `aishub.net`
[10] `github.com/dma-ais`

REFERENCES

[1] W. Abouarghoub and J. Haider, "Shipping economics: Status and future prospects," in *Contemporary Operations and Logistics*. Springer, 2019, pp. 259–279.

[2] M. Gill, "Ever given aftermath prompts re-evaluation of supply lines," Global Conversations, 2021.

[3] European Maritime Safety Agency, "Annual overview of marine casualties and incidents 2021," Tech. Rep., 2021.

[4] S. Guo, X. Zhang, Y. Zheng, and Y. Du, "An autonomous path planning model for unmanned ships based on deep reinforcement learning," *Sensors*, vol. 20, no. 2, 2020.

[5] R. Zhang, X. Wang, K. Liu, X. Wu, T. Lu, and C. Zhaohui, "Ship collision avoidance using constrained deep reinforcement learning," *Proc. of the Int. Conf. on Behavioral, Economic, and Socio-Cultural Computing*, pp. 115–120, 2018.

[6] L. Zhao, M.-I. Roh, and S.-J. Lee, "Control method for path following and collision avoidance of autonomous ship based on deep reinforcement learning," *Journal of Marine Science and Technology*, vol. 27, no. 4, pp. 293–310, 2019.

[7] A. Lazarowska, "A trajectory base method for ship's safe path planning," *Procedia Computer Science*, vol. 96, pp. 1022–1031, 2016.

[8] H. T. L. Chiang and L. Tapia, "COLREG-RRT: An RRT-based COLREGS-compliant motion planner for surface vehicle navigation," *IEEE Robotics and Automation Letters*, vol. 3, no. 3, pp. 2024–2031, 2018.

[9] K. Bergman, O. Ljungqvist, J. Linder, and D. Axehill, "An optimization-based motion planner for autonomous maneuvering of marine vessels in complex environments," in *Proc. of the IEEE Conf. on Decision and Control*, 2020, pp. 5283–5290.

[10] M. Althoff, M. Koschi, and S. Manzinger, "CommonRoad: Composable benchmarks for motion planning on roads," in *Proc. of the IEEE Intelligent Vehicles Symposium*, 2017, pp. 719–726.

[11] E. Vinitsky, A. Kreidieh, L. L. Flem, N. Kheterpal, K. Jang, C. Wu, F. Wu, R. Liaw, E. Liang, and A. M. Bayen, "Benchmarks for reinforcement learning in mixed-autonomy traffic," in *Proc. of the Conf. on Robot Learning*, 2018, pp. 399–409.

[12] L. Fan, Y. Zhu, J. Zhu, Z. Liu, O. Zeng, A. Gupta, J. Creus-Costa, S. Savarese, and L. Fei-Fei, "SURREAL: Open-source reinforcement learning framework and robot manipulation benchmark," in *Proc. of the Conf. on Robot Learning*, 2018, pp. 767–782.

[13] S. James, Z. Ma, D. R. Arrojo, and A. J. Davison, "RLBench: The robot learning benchmark & learning environment," *IEEE Robotics and Automation Letters*, vol. 5, no. 2, pp. 3019–3026, 2020.

[14] M. Moll, I. A. Sucan, and L. E. Kavraki, "Benchmarking motion planning algorithms: An extensible infrastructure for analysis and visualization," *IEEE Robotics Automation Magazine*, vol. 22, no. 3, pp. 96–102, 2015.

[15] Y. Kang, H. Yin, and C. Berger, "Test your self-driving algorithm: An overview of publicly available driving datasets and virtual testing environments," *IEEE Transactions on Intelligent Vehicles*, vol. 4, no. 2, pp. 171–185, 2019.

[16] L. Claussmann, M. Revilloud, D. Gruyer, and S. Glaser, "A review of motion planning for highway autonomous driving," *IEEE Transactions on Intelligent Transportation Systems*, vol. 21, no. 5, pp. 1826–1848, 2020.

[17] K. Tong, Z. Ajanovic, and G. Stettinger, "Overview of tools supporting planning for automated driving," in *Proc. of the IEEE Int. Conf. on Intelligent Transportation Systems*, 2020.

[18] N. Raju and H. Farah, "Evolution of traffic microsimulation and its use for modeling connected and automated vehicles," *Journal of Advanced Transportation*, vol. 2021, no. 2444363, 2021.

[19] R. Kidd, "An open-source autonomous vessel for maritime research," in *ASEE Virtual Annual Conference Content Access*, 2020.

[20] H. Krasowski and M. Althoff, "Temporal logic formalization of marine traffic rules," in *Proc. of the IEEE Intelligent Vehicles Symposium*, 2021, pp. 186–192.

[21] "COLREGs: Convention on the international regulations for preventing collisions at sea," International Maritime Organization (IMO), 1972.

[22] W. Zhang, F. Goerlandt, P. Kujala, and Y. Wang, "An advanced method for detecting possible near miss ship collisions from AIS data," *Ocean Engineering*, vol. 124, pp. 141–156, 2016.

[23] T. I. Fossen, *Handbook of Marine Craft Hydrodynamics and Motion Control*. John Wiley & Sons, Ltd, 2011.

[24] X. Zhang, C. Wang, Y. Liu, and X. Chen, "Decision-making for the autonomous navigation of maritime autonomous surface ships based on scene division and deep reinforcement learning," *Sensors*, vol. 19, no. 18, 2019.

[25] H. Yasukawa and Y. Yoshimura, "Introduction of MMG standard method for ship maneuvering predictions," *Journal of Marine Science and Technology*, vol. 20, pp. 37–52, 2015.

[26] T. I. Fossen, "How to incorporate wind, waves and ocean currents in the marine craft equations of motion," *IFAC Proceedings Volumes*, vol. 45, no. 27, pp. 126–131, 2012.

[27] R. Skjetne, O. Smogeli, and T. I. Fossen, "Modeling, identification, and adaptive maneuvering of CyberShip ii: A complete design with experiments," *IFAC Proceedings Volumes*, vol. 37, no. 10, pp. 203–208, 2004.

[28] Y. Liu, Y. Xue, S. Huang, G. Xue, and Q. Jing, "Dynamic model identification of ships and wave energy converters based on semi-conjugate linear regression and noisy input gaussian process," *Journal of Marine Science and Engineering*, vol. 9, no. 2, 2021.

[29] E. Tu, G. Zhang, L. Rachmawati, E. Rajabally, and G. B. Huang, "Exploiting AIS data for intelligent maritime navigation: A comprehensive survey from data to methodology," *IEEE Transactions on Intelligent Transportation Systems*, vol. 19, no. 5, pp. 1559–1582, 2018.

[30] "Marine cadastre - vessel traffic data," U.S. Coast Guard Navigation Center, Alexandria, USA, 2009 - 2021.

[31] S. Maierhofer, M. Klischat, and M. Althoff, "CommonRoad scenario designer: An open-source toolbox for map conversion and scenario creation for autonomous vehicles," in *Proc. of the IEEE Int. Conf. on Intelligent Transportation Systems*, 2021, pp. 3176–3182.